Received: 15 October 2023 | Revised: 10 November 2023 | Accepted: 14 November 2023

DOI: 10.1002/psc.3559

RESEARCH ARTICLE

Journal of PeptideScience WILEY

Self-assembly of heterochiral, aliphatic dipeptides with Leu

Erica Scarel[1] | Marco De Corti[1] | Maurizio Polentarutti[2] | Giovanni Pierri[3] | Consiglia Tedesco[3] | Silvia Marchesan[1]

[1]Department of Chemical and Pharmaceutical Sciences, University of Trieste, Trieste, Italy

[2]Elettra Sincrotrone Trieste, Trieste, Italy

[3]Department of Chemistry and Biology "A. Zambelli", University of Salerno, Fisciano, Italy

Correspondence
Silvia Marchesan, Department of Chemical and Pharmaceutical Sciences, University of Trieste, 34127 Trieste, Italy.
Email: smarchesan@units.it

Funding information
University of Trieste, Grant/Award Number: FRA2023

This work describes the self-assembly behavior of heterochiral, aliphatic dipeptides, L-Leu-D-Xaa (Xaa = Ala, Val, Ile, Leu), in green solvents such as acetonitrile (MeCN) and buffered water at neutral pH. Interestingly, water plays a structuring role because at 1% v/v, it enables dipeptide self-assembly in MeCN to yield organogels, which then undergo transition towards crystals. Other organic solvents and oils were tested for gelation, and metastable gels were formed in tetrahydrofuran, although at high peptide concentration (80 mM). Single-crystal X-ray diffraction revealed the dipeptides' supramolecular packing modes in amphipathic layers, as opposed to water channels reported for the homochiral Leu–Leu, or hydrophobic columns reported for homochiral Leu–Val and Leu–Ile.

KEYWORDS
chirality, crystals, D-amino acids, gels, peptides

1 | INTRODUCTION

Over the last 20 years, dipeptides have become very popular cheap building blocks for nanostructured hydrogels or organogels for a variety of applications.[1] They were reported to self-assemble into various types of nanostructures, of which the nanotubes and microtubes formed by Phe–Phe are the most popular.[2] Dipeptide gels typically consist of a matrix of elongated nanostructures, such as nanotubes and nanofibrils,[1] although dipeptides can form also other types of nanomorphologies, such as nanoparticles[3] or beaded strings.[4] Among the many types of gels that can be formed, organogels and hydrogels differ for the nature of the liquid-phase used, which is organic in the former and aqueous in the latter. Although hydrogels are certainly attractive for their sustainability, organogels can also offer a number of advantages, such as the higher variety of potential solvents (including green options, such as acetonitrile) as well as various properties (e.g., conductivity, stability, absorption and release of molecules, responsiveness) towards many advanced applications, spanning from batteries to sensors and actuators, anti-fouling or ice-phobic coatings, and so on.[5]

Numerous examples of peptide gelators are based on aromatic units to favor self-assembly in polar solvents,[6] although exceptions do exist.[7] It is widely known that aromatic N-caps are convenient appendages to favor self-organization in water through π-π stacking,[8] and Phe stands out among amino acids for its strong propensity towards self-assembly into nanostructures.[9] However, examples of non-aromatic dipeptides with free termini that self-organize into gels have appeared in lower numbers in the literature.[10–12]

During the last decade, we have investigated the introduction of D-amino acids especially in uncapped tripeptides to control the positioning of the side chains of hydrophobic amino acids, so as to attain amphiphilic conformers that can self-organize into gelling superstructures in water.[13,14] In recent years, we extended the concept to dipeptides containing Phe, and realized that the sequence space of heterochiral, aliphatic dipeptides' self-assembly is still unexplored.[12] Given that heterochiral dipeptides based on Leu and Phe revealed to be gelators regardless of the relative position of each amino acid in the sequence,[15] we chose to explore non-aromatic dipeptides, L-Leu-D-Xaa (Xaa = Ala, Val, Ile, Leu), for their ability to gel green solvents, such as buffered water or acetonitrile (MeCN). The choice fell on aliphatic hydrophobic amino acids for two reasons: first, they are more likely to yield dipeptides with sufficient hydrophobicity to self-assemble and gel; second, they would enable to fill an existing gap on the sequence-

mapping of aliphatic, hydrophobic dipeptides for their ability to self-assemble into gels and/or form water-filled nanotubes.[12]

2 | MATERIALS AND METHODS

2.1 | Materials and general methods

All solvents and reagents were obtained from Merck (Milan, Italy) and were used as provided. A 2-chlorotrytil chloride resin was bought from GL Biochem (Shanghai, China). All buffers and aqueous solutions were prepared by using pure water that was dispensed from a Millipore MilliQ-system RiOs/Origin (St. Louis, MS, USA) with a resistivity > 18.2 MΩ·cm at 25 °C. ^{1}H- and ^{13}C-nuclear magnetic resonance (NMR) spectra were recorded on a Varian Innova spectrometer at 400 and 100 MHz, respectively, while LC–MS data were obtained with an Agilent 6120 Infinity.[14] Optical microscopy images were acquired on a ZEN Primovert optical microscope with an Axiocam and a polarized filter, using Zen 3.3 (blue edition) software.

2.2 | Dipeptide synthesis and purification

The dipeptides were prepared by solid-phase peptide synthesis, using Fmoc-protection strategy and 2-chlorotrytil chloride resin, and a piperidine solution 20% in dimethylformamide (DMF). Deprotection was performed with two cycles of 7 min each. After that time, the resin was washed with dichloromethane (DCM) and DMF several times, and the deprotection was confirmed by bromophenol blue and chloranil tests. For the coupling steps, the resin was reacted with 4 equivalents of diisopropylcarbodiimide (DIC), 4 equivalents of Oxyma B, and 4 equivalents of the Fmoc-amino acid. All reactants were dissolved in DMF and then added to the resin. The reaction was kept under mixing for 1 h and 30 min. After that time, the resin was washed with DCM and DMF several times, and the coupling was confirmed by bromophenol blue and chloranil tests. Finally, the cleavage cocktail was composed of 49.5% trifluoroacetic acid (TFA), 49.5% DCM, 0.5% milliQ water, 0.5% triisopropyl silane (TIPS). The cleavage cocktail was added to the resin, and the reaction was kept under mixing for 2 h. The crudes were dissolved in 90% water with 10% MeCN, both with 0.05% TFA, and the mixtures were centrifuged at 6,000 rpm for 10 min and filtered (0.45 μm). The filtrates were purified by high-performance liquid chromatography (HPLC) in reverse phase (Agilent 1260 Infinity) on a C-18 column (Phenomenex Kinetex, 5 μm, 100 Å, 250 × 10 mm), with a gradient of acetonitrile (MeCN)/water with 0.05% TFA that was optimized for each dipeptide. L-Leu-D-Ala: t = 0–2 min, 5% MeCN; t = 15 min, 27% MeCN; t = 20–22 min, 95% MeCN; L-Leu-D-Val: t = 0–3 min, 10% MeCN; t = 17 min, 30% MeCN; t = 20–22 min, 95% MeCN; L-Leu-D-Ile: t = 0–10 min, 10% MeCN; t = 25 min, 40% MeCN; t = 28–30 min, 95% MeCN; L-Leu-D-Leu: t = 0–2 min, 5% MeCN; t = 15 min, 27% MeCN; t = 18–20 min, 95% MeCN. The products were freeze-dried into white powders. ^{1}H- and ^{13}C-NMR spectra and electrospray ionization mass spectrometry (ESI-MS) spectra confirmed products identity and purity (Supporting information S1). LC–MS analyses were performed on all the dipeptides using an analytical Agilent 6120 Infinity system (Luna, 5 μm, 100 Å, 150 × 2 mm, Phenomenex) with a quadrupole ESI-MS detector, by dissolving the dipeptides in a 1:1 mixture of MeCN/water with 0.05% formic acid and then by employing the following gradient: t = 0 min, 5% MeCN; t = 20 min, 95% MeCN; the corresponding t_R (and their %MeCN) using this method on all peptides are reported in Table 1.

2.3 | Gelation and oscillatory rheology

The dipeptides were dissolved (20 mM or 30 mM) in MeCN (or other organic solvents), and subsequent addition of 1% v/v of milliQ water with NaOH (equimolar to the peptide) led to gelation. The viscoelastic properties of the gels were probed using an oscillatory rheometer (Kinexus Ultra Plus), using a parallel-steel geometry (20-mm flat plates). In a typical experiment, the dipeptides were dissolved in the desired concentration (30 mM) of MeCN (400 μl). Before the analysis, 6 μl of 2 M NaOH were added to the solution, mixed with a pipette two times, and then the sample was transferred onto the rheometer parallel-plate (20 mm). Frequency sweeps were performed at 1 Pa while stress sweeps were recorded a frequency of 1 Hz, at 25 °C using the Peltier temperature-controller accessory of the rheometer.

2.4 | Circular dichroism

Circular dichroism (CD) spectra were recorded on freshly prepared samples (1 mM) in quartz cells (1 mm) in milliQ water with the pH adjusted to 7.0 with 0.1 M NaOH. The temperature was set at 25 °C on a Jasco J-815 with a scanning rate of 50 nm/min and a set resolution of 1 nm.

TABLE 1 L-Leu-D-Xaa (Xaa = Ala, Val, Ile, Leu) dipeptides theoretical and experimental hydrophobicity.

Peptide sequence	logP[a]	logP[b]	HPLC t_R (min)	HPLC %B[c]	Solubility (M) (ESOL)[b]	Solubility (M) (Ali)[b]	Solubility (M) (SILICOS-IT)[b]
L-Leu-D-Ala	−0.32	−1.41	12.7	60	11.3	19.9	24.4
L-Leu-D-Val	0.57	−0.84	12.8	61	3.06	3.48	$8.89 \cdot 10^{-2}$
L-Leu-D-Ile	0.98	−0.52	14.1	67	1.61	1.31	$3.52 \cdot 10^{-2}$
L-Leu-D-Leu	0.92	−0.49	14.1	67	1.24	0.85	$3.52 \cdot 10^{-2}$

Abbreviations: HPLC, high-performance liquid chromatography.
[a]Values calculated using ChemDraw Professional 15.0.0.106.
[b]Values calculated using Swiss ADME (www.SwissADME.ch).
[c]%B refers to the corresponding percentage of eluent B (MeCN) in the HPLC analytical method at t_R.

2.5 | Crystallization

The dipeptides were dissolved (20 mM) in MeCN, and subsequent addition of 1% v/v of milliQ water with NaOH (equimolar to the peptide) led to the formation of crystals of the zwitterionic peptide form that were collected after 24 h. The peptides were crystallized also in dimethyl sulfoxide (DMSO) and the structures were identical. Details of single-crystal X-ray diffraction (XRD) performed at the XRD1 beamline at Elettra synchrotron (Italy) can be found in the Supporting information S1.

3 | RESULTS AND DISCUSSION

3.1 | Dipeptides preparation and purification

The four dipeptides with the general sequence L-Leu-D-Xaa (Xaa = Ala, Val, Ile, Leu) shown in Scheme 1 were obtained in solid phase with a standard procedure using Fmoc as N-protecting group and 2-chlorotrytil chloride resin. They were purified by HPLC in reverse phase, and their purity and identity were confirmed by ESI-MS, ^{1}H- and ^{13}C-NMR spectroscopy (see Supporting information S1). Their HPLC retention times can be used as an experimental measure of their hydrophobicity,[16] and they are shown in Table 1 together with their logP. Interestingly, the HPLC retention times revealed that L-Leu-D-Ala and L-Leu-D-Val had analogous hydrophobicity, which was significantly lower than L-Leu-D-Leu and L-Leu-D-Ile. Hydrophobicity is indeed one important parameter to determine self-aggregation propensity in polar solvents.[11]

3.2 | Dipeptides characterization and self-assembly

The CD spectra of the four dipeptides were recorded in milliQ water at neutral pH to gain insights into their conformations (Figure 1).[17]

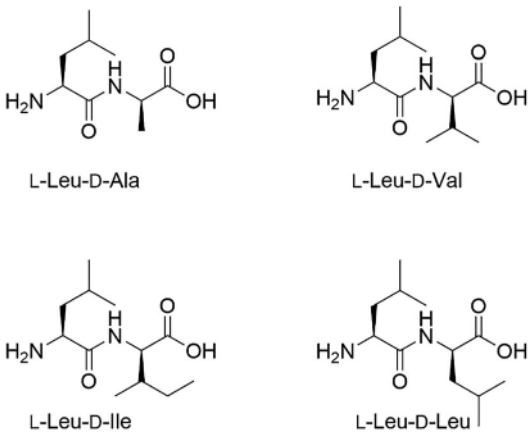

SCHEME 1 Chemical structures of the four heterochiral dipeptides studied in this work.

They were all very similar. In particular, the CD spectra of L-Leu-D-Ala, L-Leu-D-Val, and L-Leu-D-Ile presented a positive maximum centered at 197–198 nm, followed by a negative minimum at 228 nm. Analogously, the CD spectrum of L-Leu-D-Leu displayed a maximum centered at 195 nm, and a minimum at 225 nm, with the intensity of the CD signal being the lowest of the series.

The CD spectrum of L-Ala, L-Val, L-Ile, and L-Leu amino acids are characterized by a positive maximum at approximately 200 nm, which has been ascribed to the higher-energy $\pi \rightarrow \pi^*$ transition of the carbonyl group chromophore.[18] Their mirror-image enantiomers, that is,

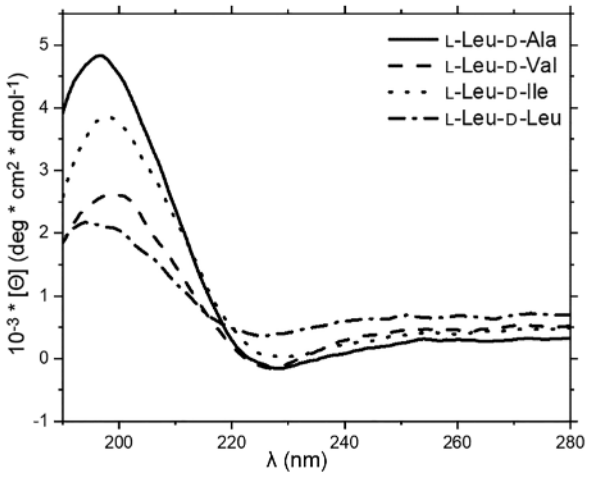

FIGURE 1 Circular dichroism (CD) spectra of the four dipeptides at 1 mM in milliQ water at pH 7.0.

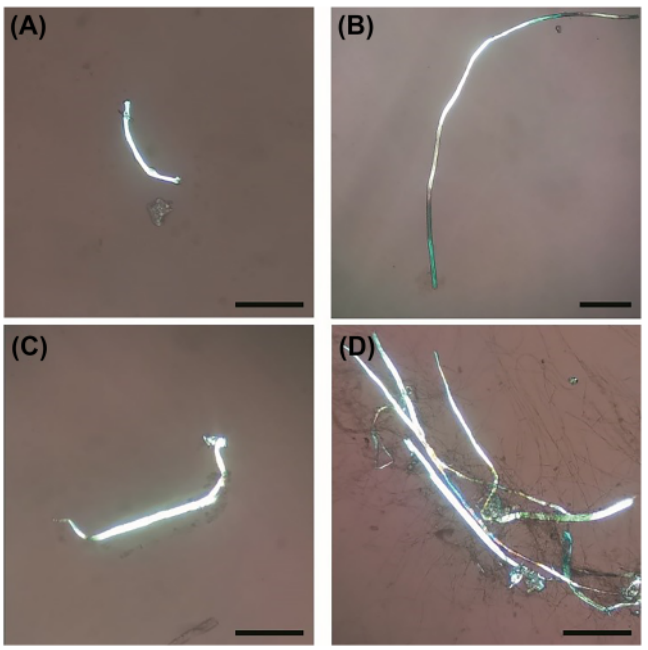

FIGURE 2 Optical microscopy photographs using a polarized filter of the dipeptide fibrils in phosphate buffer at pH 7.3. (A) L-Leu-D-Ala; (B) L-Leu-D-Val; (C) L-Leu-D-Ile; (D) L-Leu-D-Leu. Scalebar = 200 microns.

D-Ala, D-Val, D-Ile, and D-Leu, thus display a mirrored spectrum that is reflected on the y axis, thus with a negative minimum in the same region.[19] However, in the case of aliphatic dipeptides, such as L-Ala-L-Ala, the situation is inverted.[20] Furthermore, the presence of a lower-energy n → π* transition of the amide chromophore of the peptidic bond can lead to a signal in the 210–230 nm range.[21] This signal was reported to be positive for aliphatic L-dipeptides and negative for heterochiral dipeptides L-Ala-D-Xaa (Xaa = Arg, Asp, Glu, Lys, Met).[22] We can conclude that the presence of D-amino acids at the C-terminal position of aliphatic dipeptides (see also Figure 1) results in spectral features typical of aliphatic D-dipeptides, and in our case the spectra correspond to those reported for random coils. The observation of the C-terminal amino acid dictating the CD spectra chirality was in agreement with the fact that D-Phe-L-Phe displayed analogous spectral features as L-Phe-L-Phe.[23] However, care should be taken before generalizing this finding to other peptidic sequences, for it was found that in the case of dipeptide regio- and stereo-isomers containing Phe and an aliphatic amino acid (i.e., Val,[24] Leu,[25] or Ile[26]), it was the stereoconfiguration of Phe that dictated the chirality (i.e., the sign) of the CD spectral features, regardless of its position along the sequence (i.e., at the N- or C-terminus).

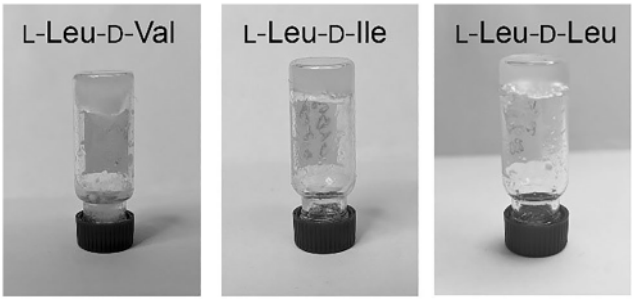

FIGURE 3 Photographs of dipeptide organogels at 20 mM in MeCN with 1% v/v water.

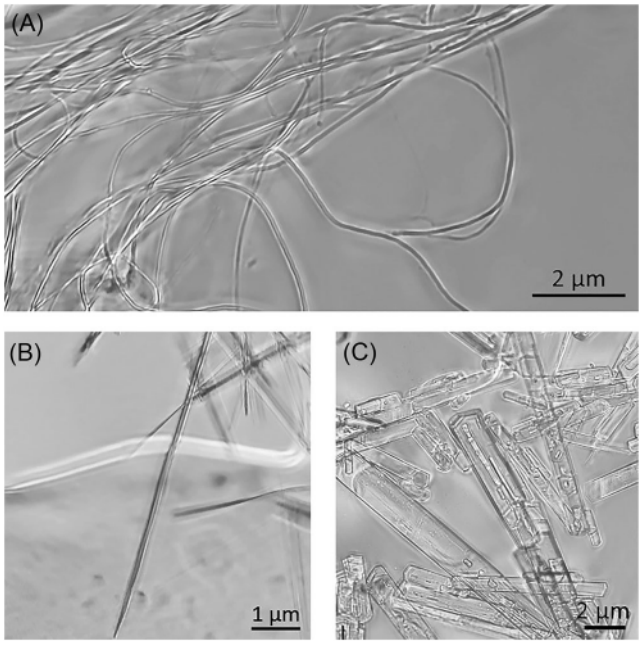

FIGURE 4 Optical microscopy photographs of (A) L-Leu-D-Leu fibrils, which then converted into (B) needle crystals, while the other dipeptides' crystals displayed different morphology, such as (C) L-Leu-D-Val crystals.

3.3 | Dipeptides self-assembly

Self-assembly of the four dipeptides was firstly probed using an established protocol.[14] Briefly, the aliphatic sequences were first dissolved in their anionic form in an alkaline solution of sodium phosphate at pH 11.8, whereby the dipeptides' negative charge at the C-terminus ensures molecular repulsion. Next, lowering the pH to neutral through the addition of an equal volume of a mildly acidic

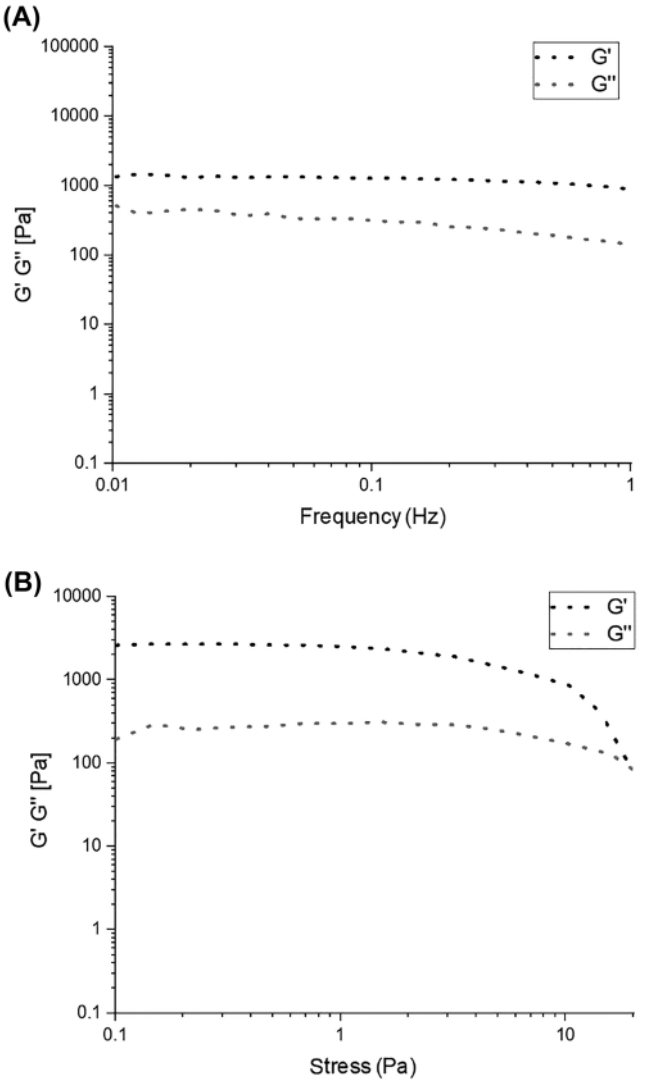

FIGURE 5 Oscillatory rheology of L-Leu-D-Leu organogel. (A) Frequency sweep, (B) stress sweep.

sodium phosphate buffer typically triggers self-assembly of the zwitterions that can engage in electrostatic interactions between the positively charged N-termini and the anionic carboxylates at the C-termini. In all cases, rare instances of microfibrils were observed by optical microscopy (Figure 2), although they were very short and thin in the case of the least hydrophobic L-Leu-D-Ala, and progressively more visible for L-Leu-D-Val and L-Leu-D-Ile and especially longer for L-Leu-D-Leu.

In acetonitrile (MeCN), all the four dipeptides were completely soluble even at the high concentration of 20 mM. However, it was sufficient to add just 1% v/v of milliQ water with an amount of NaOH that was equimolar to the dipeptides (to neutralize the presence of TFA from the HPLC purification and obtain the zwitterions) to induce organogelation of the three dipeptides (Figure 3) L-Leu-D-Val (minimum gelling concentration, mgc, 30 mM), L-Leu-D-Ile (mgc 20 mM), and L-Leu-D-Leu (mgc 20 mM). For comparison, (*p*-aminobenzoyl)-L-Phe-D-Ala-L-Phe-NH_2 also displayed an mgc of 30 mM in MeCN.[26] Other solvents were also tested following the same procedure, but the dipeptides were highly soluble in alcohols (methanol or ethanol), insoluble in soybean or silicone oil. In DMSO, they all crystallized. L-Leu-D-Leu and L-Leu-D-Ile gelled tetrahydrofuran, but at the high concentration of 80 mM.

After 24 h, in all cases the metastable organogels in MeCN underwent a transition towards crystals. Only in the case of L-Leu-D-Leu, curved fibrils were firstly seen by optical microscopy (Figure 4A), before transitioning towards needle crystals (Figure 4B). Conversely, in all the other cases, crystals rapidly formed with different morphologies (Figure 4C). The evolution from gels to crystals is a relatively common phenomenon in peptide self-assembly, whose kinetics and thermodynamics have been widely studied,[27] although exceptions do exist with gels representing the thermodynamic product.[28]

3.4 | Dipeptide organogel characterization

Oscillatory rheometry is the most appropriate technique to assess the viscoelastic properties of soft matter and confirm the gel nature. However, in the case of all peptides, but L-Leu-D-Leu, the transition towards crystals inevitably started during the rheological analyses, leading to extensive noise and impeding correct measurements. Therefore, only the rheological analyses of the L-Leu-D-Leu organogel in MeCN are reported in Figure 5. In particular, it was not possible to monitor the gelation kinetics, which occurred immediately after the addition of water as described in the previous section. Subsequent frequency sweeps confirmed a soft gel nature with the storage (G′) and loss (G″) moduli corresponding to 1.6 ± 0.5 kPa and 0.3 ± 0.1 kPa, respectively, which were not dependent upon the applied frequency in the range of 0.1–10 Hz (Figure 5A). Furthermore, stress sweeps showed a linear viscoelastic interval until 1 Pa, and a subsequent sol–gel transition at approximately 20 Pa (Figure 5B).

TABLE 2 Intermolecular distances (Å) and angles (°) for the selected hydrogen bonds found in the crystal structures of the four dipeptides.

Crystal structure	D-H···A	D···A (Å)	H···A (Å)	∠D-H···A (°)
L-Leu-D-Ala	N1-H1A···O1W	2.725(2)	1.80(2)	172(2)
	N1-H1B···O2	2.961(1)	2.11(2)	151(2)°
	N1-H1C···O3	2.830(1)	1.96(3)	169(2)
	N2-H2···O1	2.952(1)	2.19(3)	162(2)
	C1-H1···O1	3.118(1)	2.18	155
	O2W-H2WA···O3	2.771(2)	1.93(2)	167(2)
	O2W-H2WB···O3	2.757(1)	1.91(2)	171(2)
L-Leu-D-Val	N1-H1A···O3W	2.79	1.88	175
	N1-H1B···O1W	2.867(1)	2.11(3)	165(3)
	N1-H1C···O2W	2.75(1)	1.88(3)	169(3)
L-Leu-D-Leu	N1-H1A···O1S	2.84(2)	1.94(4)	171(3)
	N1-H1B···O2	2.750(8)	1.97(4)	161(4)
	N1-H1C···O3	2.77(2)	1.83(5)	171(3)
L-Leu-D-Ile	N1A-H1AA···O1S	2.83(1)	1.92(3)	173(3)
	N1A-H1AB···O3A	2.751(4)	1.85(3)	169(3)
	N1A-H1AC···O2A	2.79(1)	1.87(3)	172(3)
	N1B-H1BA···O2S	2.802(8)	1.87(3)	169(3)
	N1B-H1BB···O3B	2.710(4)	1.79(3)	174(3)
	N1B-H1BC···O2B	2.78(1)	1.86(3)	174(3)

3.5 | XRD analyses

The single crystals obtained from the hydrogels as described above in Sections 2.5 and 3.2 were analyzed by XRD using synchrotron radiation (see Supporting information S1). The intermolecular distances and angles for the hydrogen bonds found in the crystal structures of the four dipeptides are listed in Table 2.

L-Leu-D-Ala (CCDC deposition number 2300851) crystallizes as a hydrate crystal form with a host: guest ratio of 1:2 (Figure 6). In contrast to the homochiral counterpart crystal structure, which is characterized by water channels,[29] in the crystal structure of L-Leu-D-Ala water molecules are localized in layers parallel to the *ab* plane. Regarding the intermolecular interactions, L-Leu-D-Ala shows two hydrogen atoms of the $-NH_3^+$ groups interacting with the $^-OOC-$ whereas the third hydrogen atom interacts with water molecules O1W localized inside the channel. Additionally, the dipeptides align one on top of the other along the *b* axis via hydrogen bonds involving the carbonyl oxygen atom O1, the hydrogen atom of the peptide bond and the hydrogen atom attached to the α-carbon. These two motifs promote the formation of amphipathic layers, which are separated into hydrophobic and hydrophilic regions defined by the side chains and backbone atoms, respectively. The latter contains the water molecules that interact with the dipeptides.

Analogously, L-Leu-D-Val (CCDC deposition number 2300852) crystallizes as a hydrate crystal form with a host:guest ratio of 1:2.5, but in this case, water molecules occupy non-interconnected cavities (Figure 7). Crystals were obtained also in DMSO, and the structure

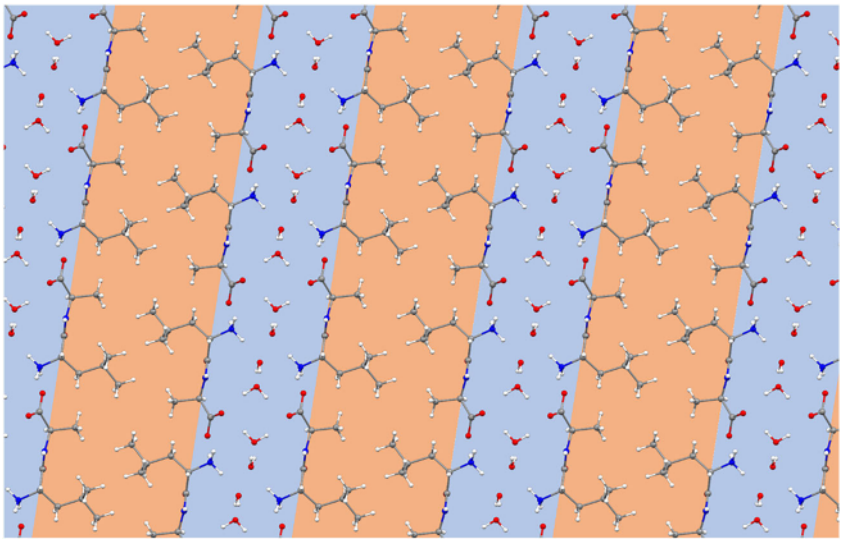

FIGURE 6 Crystal packing of L-Leu-D-Ala (view along the *b* axis). Hydrophilic regions in light blue background, hydrophobic regions in light orange background. Atom types: C gray, H white, O red, N blue. Only the atoms with the highest occupancy factors are shown.

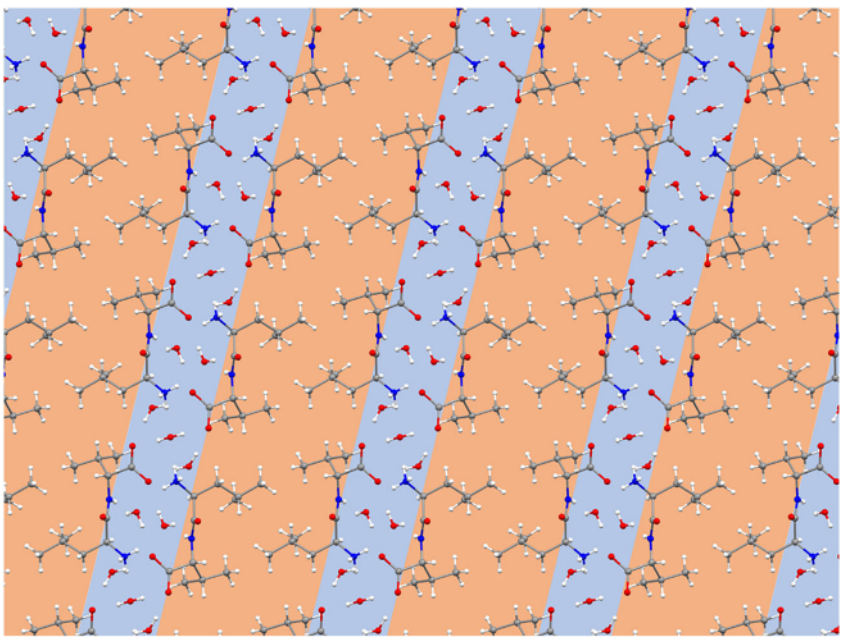

FIGURE 7 Crystal packing of L-Leu-D-Val (view along the *b* axis). Hydrophilic regions in light blue background, hydrophobic regions in light orange background. Atom types: C gray, H white, O red, N blue.

was identical. Another difference between the solid-state assemblies of the two dipeptides emerges from the intermolecular interactions' analysis. As already reported for the solid-state assembly of the dipeptide D-Val-L-Phe,[24] in L-Leu-D-Val the $-NH_3^+$ and $^-OOC-$ groups directly interact with the water molecules that connect the dipeptides, and no host–host hydrogen bonds can be highlighted. With respect to the hydrate crystal structure of the homochiral dipeptide L-Leu-L-Val reported by Görbitz,[30] which shows a peculiar crystal packing with Z = 24, L-Leu-D-Val is characterized by a quite simple solid-state assembly. In particular, dipeptides form amphipathic layers with a hydrophilic region in which are present the water molecules, defined by the backbone atoms and a hydrophobic region defined by the side chains.

Single crystals of suitable quality for XRD analysis were obtained for both L-Leu-D-Leu and L-Leu-D-Ile in DMSO (CCDC deposition numbers 2300853 and 2300854, respectively). Both dipeptides crystallize as DMSO solvate crystal structures with the guest molecules which occupy channels parallel to the *a* axis (Figure 8). The crystal

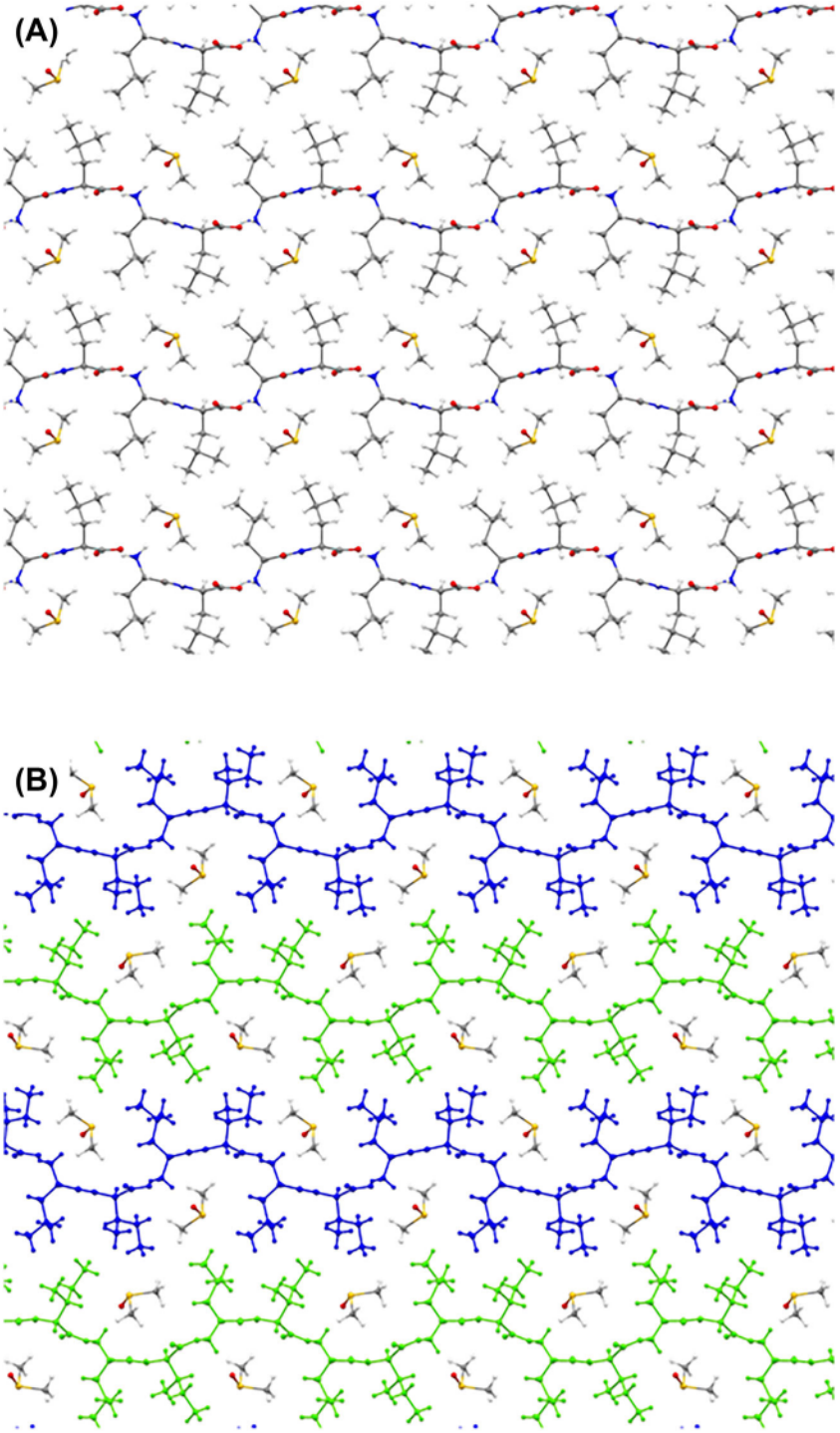

FIGURE 8 (A) Crystal packing of L-Leu-D-Leu (view along the *a* axis). (B) Crystal packing of L-Leu-D-Ile (view along the *a* axis). The two independent dipeptide molecules in the asymmetric unit are depicted in green and blue. Atom types: C gray, H white, O red, N blue, S yellow.

packing analysis performed on the two crystal structures reveals a very similar solid-state arrangement with the dipeptides forming a layered structure with channels surrounded by the hydrophobic side chains. L-Leu-D-Ile, in contrast to L-Leu-D-Leu, shows two independent dipeptide molecules in the asymmetric unit and two interconnected channels where the DMSO guest molecules are localized. In both crystal structures, two of three hydrogen atoms of the $-NH_3^+$ interact head-to-tail with the $^-OOC-$ group defining the sheet structure while the third one directly interacts with the DMSO molecule localized inside the channel. Regarding the homochiral counterparts, Mitra and Subramanian[31] have reported the DMSO solvate crystal structure of L-Leu-L-Leu whereas, to the best of our knowledge, the DMSO solvate crystal structure of the dipeptide L-Leu-L-Ile has never been reported in literature.

4 | CONCLUSIONS

In conclusion, this work reports the preparation, characterization, and study of the self-assembly behavior of the four heterochiral dipeptides L-Leu-D-Xaa (Xaa = Ala, Val, Ile, Leu) in buffered water and MeCN. Water played a structuring role, for its addition to a MeCN solution of either one of the four dipeptides triggered self-assembly into metastable organogels, which then converted into crystals. The supramolecular packing of all the four compounds revealed the presence of amphipathic layers, as opposed to water-filled channels observed for other self-assembling hydrophobic dipeptides with Leu.[15] However, it should be noted that the crystals of L-Leu-D-Leu and L-Leu-D-Ile were obtained in DMSO, which is also present in the crystal structure, and it is possible that in water a different packing can be found. This work adds another piece to the puzzle of heterochiral dipeptide self-assembly[12] to complete the mapping of the nanostructures obtained by these simple building blocks towards functional and green materials. Potential applications could include molecular and solvent separation and environmental remediation,[32] on their own or together with other components in smart materials.[33]

ACKNOWLEDGEMENTS

The authors are grateful to the University of Trieste for funding support (FRA2023) and to Elettra Sincrotrone Trieste for providing access to its synchrotron radiation facilities and, in particular, to the XRD1 beamline.

ORCID

Giovanni Pierri https://orcid.org/0000-0001-5433-6077
Silvia Marchesan https://orcid.org/0000-0001-6089-3873

REFERENCES

1. Castilla AM, Dietrich B, Adams DJ. Using aggregation-induced emission to understand dipeptide gels. *Gels*. 2018;4(1):17. doi:10.3390/gels4010017 Chakraborty P, Tang Y, Yamamoto T, et al. Unusual two-step assembly of a minimalistic dipeptide-based functional hypergelator. *Adv Mater*. 2020;32(9):e1906043. doi:10.1002/adma.201906043 Fuentes-Caparrós AM, McAulay K, Rogers SE, Dalgliesh RM, Adams DJ. On the mechanical properties of N-functionalised dipeptide gels. *Molecules*. 2019;24(21):3855. doi:10.3390/molecules24213855 Halder M, Bhatia Y, Singh Y. Self-assembled di- and tripeptide gels for the passive entrapment and pH-responsive, sustained release of an antidiabetic drug, glimepiride. *Biomater Sci*. 2022;10(9):2248-2262. doi:10.1039/D2BM00344A Hill MJS, Adams DJ. Multi-layer 3D printed dipeptide-based low molecular weight gels. *Soft Matter*. 2022;18(32):5960-5965. doi:10.1039/D2SM00663D Kumar M, Sementa D, Narang V, Riedo E, Ulijn RV. Self-assembly propensity dictates lifetimes in transient naphthalimide–dipeptide nanofibers. *Chem – Eur J*. 2020;26(38):8372-8376. doi:10.1002/chem.202001008 Li F, Han J, Cao T, et al. Design of self-assembly dipeptide hydrogels and machine learning via their chemical features. *Proc Natl Acad Sci U S A*. 2019;116(23):11259-11264. doi:10.1073/pnas.1903376116 Oliveira CBP, Pereira RB, Pereira DM, et al. Aryl-capped lysine-dehydroamino acid dipeptide supergelators as potential drug release systems. *Int J Mol Sci*. 2022;23(19):11811. doi:10.3390/ijms231911811
2. Reches M, Gazit E. Casting metal nanowires within discrete self-assembled peptide nanotubes. *Science*. 2003;300(5619):625-627. doi:10.1126/science.1082387
3. Sivagnanam S, Das K, Basak M, et al. Self-assembled dipeptide based fluorescent nanoparticles as a platform for developing cellular imaging probes and targeted drug delivery chaperones. *Nanoscale Adv*. 2022;4(6):1694-1706. doi:10.1039/D1NA00885D
4. Yuran S, Razvag Y, Reches M. Coassembly of aromatic dipeptides into biomolecular necklaces. *ACS Nano*. 2012;6(11):9559-9566. doi:10.1021/nn302983e
5. Kuzina MA, Kartsev DD, Stratonovich AV, Levkin PA. Organogels versus hydrogels: advantages, challenges, and applications. *Adv Funct Mater*. 2023;33(27):2301421. doi:10.1002/adfm.202301421
6. Wychowaniec JK, Smith AM, Ligorio C, Mykhaylyk OO, Miller AF, Saiani A. Role of sheet-edge interactions in β-sheet self-assembling-peptide hydrogels. *Biomacromolecules*. 2020;21(6):2285-2297. doi:10.1021/acs.biomac.0c00229 Azoulay Z, Aibinder P, Gancz A, Moran-Gilad J, Navon-Venezia S, Rapaport H. Assembly of cationic and amphiphilic β-sheet FKF tripeptide confers antibacterial activity. *Acta Biomater*. 2021;125:231-241. doi:10.1016/j.actbio.2021.02.015
7. La Manna S, Florio D, Panzetta V, et al. Hydrogelation tunability of bioinspired short peptides. *Soft Matter*. 2022;18(44):8418-8426. doi:10.1039/D2SM01385A Alshehri S, Susapto HH, Hauser CAE. Scaffolds from self-assembling tetrapeptides support 3D spreading, osteogenic differentiation, and angiogenesis of mesenchymal stem cells. *Biomacromolecules*. 2021;22(5):2094-2106. doi:10.1021/acs.biomac.1c00205 Diaferia C, Ghosh M, Sibillano T, et al. Fmoc-FF and hexapeptide-based multicomponent hydrogels as scaffold materials. *Soft Matter*. 2019;15(3):487-496. doi:10.1039/C8SM02366B Shariati Pour SR, Oddis S, Barbalinardo M, et al. Delivery of active peptides by self-healing, biocompatible and supramolecular hydrogels. *Molecules*. 2023;28(6):2528. doi:10.3390/molecules28062528
8. Tao K, Levin A, Adler-Abramovich L, Gazit E. Fmoc-modified amino acids and short peptides: simple bio-inspired building blocks for the fabrication of functional materials. *Chem Soc Rev*. 2016;45(14):3935-3953. doi:10.1039/C5CS00889A Martin AD, Thordarson P. Beyond Fmoc: a review of aromatic peptide capping groups. *J Mater Chem B*. 2020;8(5):863-877.
9. Adler-Abramovich L, Vaks L, Carny O, et al. Phenylalanine assembly into toxic fibrils suggests amyloid etiology in phenylketonuria. *Nat Chem Biol*. 2012;8(8):701-706. doi:10.1038/nchembio.1002
10. Chan KH, Lee WH, Ni M, Loo Y, Hauser CAE. C-terminal residue of ultrashort peptides impacts on molecular self-assembly, hydrogelation, and interaction with small-molecule drugs. *Sci Rep*. 2018;8(1):17127. doi:10.1038/s41598-018-35431-2

11. Frederix PWJM, Scott GG, Abul-Haija YM, et al. Exploring the sequence space for (tri-)peptide self-assembly to design and discover new hydrogels. *Nat Chem*. 2015;7(1):30-37. doi:10.1038/nchem.2122
12. Bellotto O, D'Andrea P, Marchesan S. Nanotubes and water-channels from self-assembling dipeptides. *J Mater Chem B*. 2023;11(24):5378-5389. doi:10.1039/D2TB02643K
13. Garcia AM, Melchionna M, Bellotto O, et al. Nanoscale assembly of functional peptides with divergent programming elements. *ACS Nano*. 2021;15(2):3015-3025. doi:10.1021/acsnano.0c09386
14. Parisi E, Adorinni S, Garcia AM, Kralj S, De Zorzi R, Marchesan S. Self-assembling tripeptide forming water-bound channels and hydrogels. *J Pept Sci*. 2023;29(11):e3524. doi:10.1002/psc.3524
15. Bellotto O, Kralj S, De Zorzi R, Geremia S, Marchesan S. Supramolecular hydrogels from unprotected dipeptides: a comparative study on stereoisomers and structural isomers. *Soft Matter*. 2020;16(44):10151-10157. doi:10.1039/D0SM01191F
16. Bolt HL, Williams CEJ, Brooks RV, Zuckermann RN, Cobb SL, Bromley EHC. Log *D* versus HPLC derived hydrophobicity: the development of predictive tools to aid in the rational design of bioactive peptoids. *Biopolymers*. 2017;108(4):e23014. doi:10.1002/bip.23014
17. Pignataro MF, Herrera MG, Dodero VI. Evaluation of peptide/protein self-assembly and aggregation by spectroscopic methods. *Molecules*. 2020;25(20):4854. doi:10.3390/molecules25204854
18. Amdursky N, Stevens MM. Circular dichroism of amino acids: following the structural formation of phenylalanine. *ChemPhysChem*. 2015;16(13):2768-2774. doi:10.1002/cphc.201500260
19. Ding R, Ying J, Zhao Y. An electronic circular dichroism spectroscopy method for the quantification of L- and D-amino acids in enantiomeric mixtures. *R Soc Open Sci*. 2021;8(3):201963. doi:10.1098/rsos.201963
20. Adler-Abramovich L, Reches M, Sedman VL, Allen S, Tendler SJ, Gazit E. Thermal and chemical stability of diphenylalanine peptide nanotubes: implications for nanotechnological applications. *Langmuir*. 2006;22(3):1313-1320. doi:10.1021/la052409d
21. Nordén AR, Nordén B. *Circular dichroism and linear dichroism*. Oxford University Press; 1997.
22. Yang J, Zhong S, Chen X, et al. A direct circular dichroic assay for quantitative determination of peptide enantiomers. *iScience*. 2021;53(10):1412-1415. doi:10.1093/abbs/gmab104
23. Kralj S, Bellotto O, Parisi E, et al. Heterochirality and halogenation control Phe–Phe hierarchical assembly. *ACS Nano*. 2020;14(12):16951-16961. doi:10.1021/acsnano.0c06041
24. Bellotto O, Pierri G, Rozhin P, et al. Dipeptide self-assembly into water-channels and gel biomaterial. *Org Biomol Chem*. 2022;20(31):6211-6218. doi:10.1039/D2OB00622G
25. Bellotto O, Kralj S, Melchionna M, et al. Self-assembly of unprotected dipeptides into hydrogels: water-channels make the difference. *ChemBioChem*. 2022;23(2):e202100518. doi:10.1002/cbic.202100518
26. Kieffer M, Garcia AM, Haynes CJE, et al. Embedding and positioning of two $Fe^{II}_4L_4$ cages in supramolecular tripeptide gels for selective chemical segregation. *Angew Chem Int Ed*. 2019;58(24):7982-7986. doi:10.1002/anie.201900429
27. Wang J, Liu K, Xing R, Yan X. Peptide self-assembly: thermodynamics and kinetics. *Chem Soc Rev*. 2016;45(20):5589-5604. doi:10.1039/C6CS00176A
28. Ramos Sasselli I, Halling PJ, Ulijn RV, Tuttle T. Supramolecular fibers in gels can be at thermodynamic equilibrium: a simple packing model reveals preferential fibril formation versus crystallization. *ACS Nano*. 2016;10(2):2661-2668. doi:10.1021/acsnano.5b07690
29. Görbitz C. Cyclic water pentamers in L-leucyl-L-alanine tetrahydrate. *Acta Crystallogr C*. 1997;53(6):736-739. doi:10.1107/S0108270196015946
30. Görbitz C, Gundersen E. L-Leu-L-Val.3/4H_2O: a hexagonal crystal structure with Z = 24. *Acta Chem Scand*. 1996;50:537-543. doi:10.3891/acta.chem.scand.50-0537
31. Mitra SN, Subramanian E. Observation of a sterically unfavorable side-chain conformation in a leucyl residue: crystal and molecular structure of L-leucyl–L-leucine · DMSO solvate. *Biopolymers*. 1994;34(9):1139-1143. doi:10.1002/bip.360340903
32. Ziganshin MA, Safiullina AS, Ziganshina SA, Gerasimov AV, Gorbatchuk VV. Non-zeolitic properties of the dipeptidel-leucyl–L-leucine as a result of the specific nanostructure formation. *Phys Chem Chem Phys*. 2017;19(21):13788-13797. doi:10.1039/C7CP01393K Mondal B, Bairagi D, Nandi N, et al. Peptide-based gel in environmental remediation: removal of toxic organic dyes and hazardous Pb^{2+} and Cd^{2+} ions from wastewater and oil spill recovery. *Langmuir*. 2020;36(43):12942-12953. doi:10.1021/acs.langmuir.0c02205 Kanti Das B, Samanta R, Ahmed S, Pramanik B. Disulphide cross-linked ultrashort peptide hydrogelator for water remediation. *Chem – Eur J*. 2023;29(37):e202300312. doi:10.1002/chem.202300312 Fortunato A, Mba M. A peptide-based hydrogel for adsorption of dyes and pharmaceuticals in water remediation. *Gels*. 2022;8(10):672. doi:10.3390/gels8100672
33. Jahović I, Zou Y-Q, Adorinni S, Nitschke JR, Marchesan S. Cages meet gels: smart materials with dual porosity. *Matter*. 2021;4(7):2123-2140. doi:10.1016/j.matt.2021.04.018 Bi H, An C, Mulligan CN, et al. Application of phase-selective organogelators (PSOGs) for marine oil spill remediation. *J Mar Sci Eng*. 2022;10(8):1111. doi:10.3390/jmse10081111 Lopez-Fernandez M, Tariq S, Naseem K, et al. Graphene based composite membranes for environmental toxicology remediation, critical approach towards environmental management. *Chemosphere*. 2022;307(Pt 4):136034. doi:10.1016/j.chemosphere.2022.136034 Fortunato A, Mba M. Metal cation triggered peptide hydrogels and their application in food freshness monitoring and dye adsorption. *Gels*. 2021;7(3):85. doi:10.3390/gels7030085 Raymond DM, Nilsson BL. Multicomponent peptide assemblies. *Chem Soc Rev*. 2018;47(10):3659-3720. doi:10.1039/C8CS00115D Adorinni S,Rozhin P,Marchesan S. Smart hydrogels meet carbon nanomaterials for new frontiers in medicine. *Biomedicines*. 2021;9(5):570. doi:10.3390/biomedicines9050570

SUPPORTING INFORMATION

Additional supporting information can be found online in the Supporting Information section at the end of this article.

How to cite this article: Scarel E, De Corti M, Polentarutti M, Pierri G, Tedesco C, Marchesan S. Self-assembly of heterochiral, aliphatic dipeptides with Leu. *J Pept Sci*. 2024;30(5):e3559. doi:10.1002/psc.3559